Force Spectroscopy of an Elastic Peptide: Effect of D_2O and Temperature on Persistence Length

SIMON J. HAWARD,[1]* PETER R. SHEWRY,[2] JUSTIN MARSH,[2] MERVYN J. MILES,[1] AND TERENCE J. McMASTER[1]
[1]*H. H. Wills Physics Laboratory, University of Bristol, Tyndall Avenue, Bristol BS8 1TL, United Kingdom*
[2]*Plant Science Department, Rothamsted Research, Harpenden, Hertfordshire, AL5 2JQ, United Kingdom*

KEY WORDS AFM; single molecule stretching; protein folding; isotopic substitution

ABSTRACT This study explores the mechanical unfolding of elastic protein analogues as a function of temperature, in both H_2O and D_2O, using atomic force microscopy (AFM) force spectroscopy in a specially constructed AFM liquid cell. This represents the first time that the effect of D_2O on protein flexibility has been investigated at the single molecule level by this technique. Model elastic peptides, R6, were encoded from synthetic genes expressed in *Escherichia coli*. The peptides possess short N- and C-terminal domains with central repetitive domains containing 13 repeats of the motif PGQGQQ-plus-GYYPTSLQQ. These sequences mimic those in native high molecular weight subunit glutenin proteins which confer elasticity to bread dough. Fitting single molecule stretching events to the worm-like chain model, allows determination of the molecular persistence length under various experimental conditions. The effect of increasing the temperature is to increase the persistence length of the peptide in both H_2O and D_2O, consistent with the expected "thermal softening" effect. However, the effect is significantly enhanced in D_2O, in which the persistence length at 45°C is ~25% greater than the value measured in H_2O at the same temperature. Stronger intrapeptide H-bonding due to isotopic substitution of hydrogen for deuterium is the most likely cause of the enhanced backbone rigidity. *Microsc. Res. Tech. 74:170–176, 2011.*

INTRODUCTION

The stretching of single molecules, or force spectroscopy, by atomic force microscopy (AFM) methods is a powerful tool for the study of inter- and intramolecular interactions involving biomolecules. Examples of its use include the measurement of ligand-receptor unbinding forces (Moy et al., 1994), the direct measurement of forces between complementary DNA strands (Lee et al., 1994), and the mechanical unfolding of proteins (Rief et al., 1997).

In protein unfolding experiments, one end of a protein molecule is tethered to a solid substrate and the other end is bound to the tip of an AFM cantilever. The deflection of the cantilever is monitored as a function of the tip-substrate separation from which a force-distance curve for the molecule can be derived. All of this is ideally performed in a physiological buffer solution. The characteristic force-distance curves can be fitted with force-extension models such as the freely jointed or worm-like chain (WLC) in order to extract values for molecular parameters such as persistence length (e.g., Bouchiat et al., 1999; Bustamante et al., 1994). Forbes et al. (2005) have used these methods to find changes in the persistence length of the PEVK (Proline (P), Glutamic acid (E), Valine (V) and Lysine (K)) segment of the protein titin with variations in the ionic strength of the solvent.

Recently, reliable methods have been developed for the accurate control of the temperature of liquid samples within the AFM set-up, enabling experiments at physiological relevant temperatures and facilitating temperature dependence studies of the physiological function of biomolecules (Janovjak et al., 2003; Law et al., 2003; Schlierf and Rief, 2005; Taniguchi et al., 2008). These studies have shown a reduction in the force required for the unfolding of proteins as the temperature is increased, i.e., thermal softening of the protein structure.

Isotopic substitution of hydrogen by deuterium in the solvation shell has been demonstrated to be a stabilizing factor for polyproline II (PPII) helical structures in proteins (Chelgren and Creamer, 2004) and to cause a significant increase in the rigidity of protein structures (Cioni and Strambini, 2002). This may be because the D-bond is intrinsically stronger than the H-bond (Nemethy and Sheraga, 1964; Scheiner and Cuma, 1996) or be due to a solvent ordering effect (Markus and Ben-Naim, 1985). Cioni and Strambini (2002) found that, with increasing temperature, protein structures stiffened to a greater degree when dissolved in D_2O compared with H_2O. The reason for this was attributed to the hydrophobic nature of the interaction, as suggested by Parker and Clarke (1997). The free-energy gain of burying nonpolar amino acid residues is greater if the cohesive property of the bulk solvent is large.

Understanding the effects of D_2O on protein structures is of significant relevance to biophysical studies

*Correspondence to: Simon J. Haward, H. H. Wills Physics Laboratory, University of Bristol, Tyndall Avenue, Bristol BS8 1TL, United Kingdom.
E-mail: s.j.haward@bristol.ac.uk

Received 12 March 2010; accepted in revised form 5 May 2010

Contract grant sponsor: Biotechnology and Biological Sciences Research Council of the UK

DOI 10.1002/jemt.20888

Published online 11 June 2010 in Wiley Online Library (wileyonlinelibrary.com).

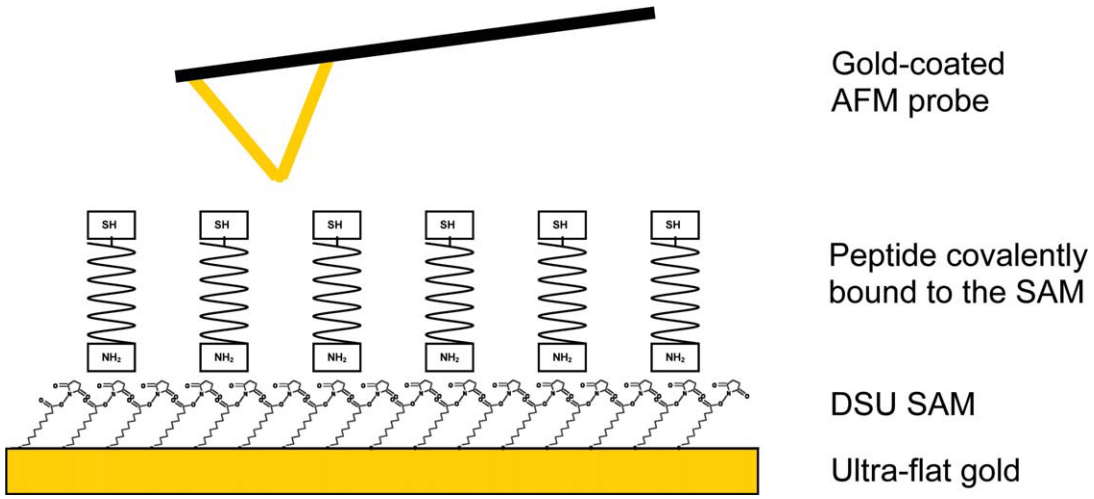

Fig. 1. Schematic of the experimental approach used to tether the R6 peptide and stretch it with the AFM. After Wagner et al. (1996). [Color figure can be viewed in the online issue, which is available at wileyonlinelibrary.com.]

involving spectroscopic techniques including NMR and Raman, which routinely solvate samples with D_2O. Single molecule AFM force spectroscopy has been used recently to study the effect of solvent hydrogen bonds on the folding/unfolding of the I27 module of titin (Dougan et al., 2008). Replacing H_2O with D_2O as the solvent had the general effect of stabilizing the protein structure, and lead to speculation that a rapid hydrogen-deuterium exchange had occurred in important regions of the molecule, strengthening the hydrogen bonds there. Dougan et al. also found D_2O was a worse solvent for I27 than H_2O, in interesting contrast with previous experiments (e.g., Markus and Ben-Naim, 1985). However, the interpretation of unfolding data from titin is complicated due to an unfolding intermediate in the protein. This results in a hump in the force-extension curves, which means they deviate from entropic elastic behavior.

In this study, we aim to further enhance our understanding of the effects of isotopic substitution of hydrogen by deuterium on the stability of protein structures. We perform single molecule force spectroscopy experiments on a model monomeric single domain repetitive elastic peptide in H_2O and D_2O based buffer solutions. D_2O based solutions are left for sufficient time before experimentation to allow full isotopic substitution to take place. Experiments are conducted at controlled temperatures of $8^{\circ}C < T < 45^{\circ}C$ allowing us to examine the combined effect of temperature and solvent on the elasticity of the peptide by determining the molecular persistence length in each case using the WLC model.

MATERIALS AND METHODS

The synthetic peptide used in this study is known as R6 and was encoded from synthetic genes expressed in *Escherichia coli*, as described (Feeney et al., 2003). It has short N and C terminal domains with central repetitive domains containing 13 repeats of the motif PGQGQQ + GYYPTSLQQ. The repetitive domain is based on the repeat sequences found in the native high molecular weight (HMW) glutenin subunits of wheat, which are the proteins largely responsible for the elastic properties of wheat dough (Shewry and Tatham, 1990). In solution, the HMW subunits, and hence the R6 peptide molecule, are expected to adopt a "β-spiral" secondary structure based on an equilibrium of β-reverse turns and poly-L-proline II-type structure (McIntire et al., 2005; Miles et al., 1991; Parchment et al., 2001).

In the R6 peptide, the sixth glutamine residue of the first repeat sequence and the last glutamine residue of the final repeat sequence have been replaced by cysteine residues. The cysteine residues provide well located and convenient binding sites for a gold-coated AFM probe. The well-defined chemistry, monodisperse molecular weight, and convenient placement of binding sites at either end of the molecule make this a model peptide for study using AFM force spectroscopy.

A schematic showing how the peptides were tethered and stretched in the AFM is provided in Figure 1. Ultra-flat "template-stripped" gold (TSG) surfaces were prepared as described by Hegner et al. (1993). The TSG surfaces were treated with a 1 mM solution of dithiobis(-succinimidylundecanoate) (DSU) in 1,4-dioxane for ~10 min, which is sufficient time for a DSU self-assembled monolayer to form on the TSG surface (Wagner et al., 1996). The DSU molecule forms a covalent thiol bond with the gold surface and leaves a succinimide group exposed. The succinimide group has a preferential affinity to covalently bind with primary amine groups.

The R6 peptide was dissolved to a concentration of 0.1 mg mL^{-1} in a solution of 20 mM sodium hydrogen carbonate ($NaHCO_3$) and 1 mM dithiothreitol (DTT) in either H_2O or D_2O. The DTT was present in the solution to prevent the formation of disulphide bonds between cysteine resides and maintain the peptide molecules as monomeric entities. The D_2O based peptide solutions were left for several days prior to experimentation to allow isotopic substitution to take place (Milne et al., 1998). Quantities of the solvents ($NaHCO_3$ in either H_2O or D_2O) were also prepared without DTT.

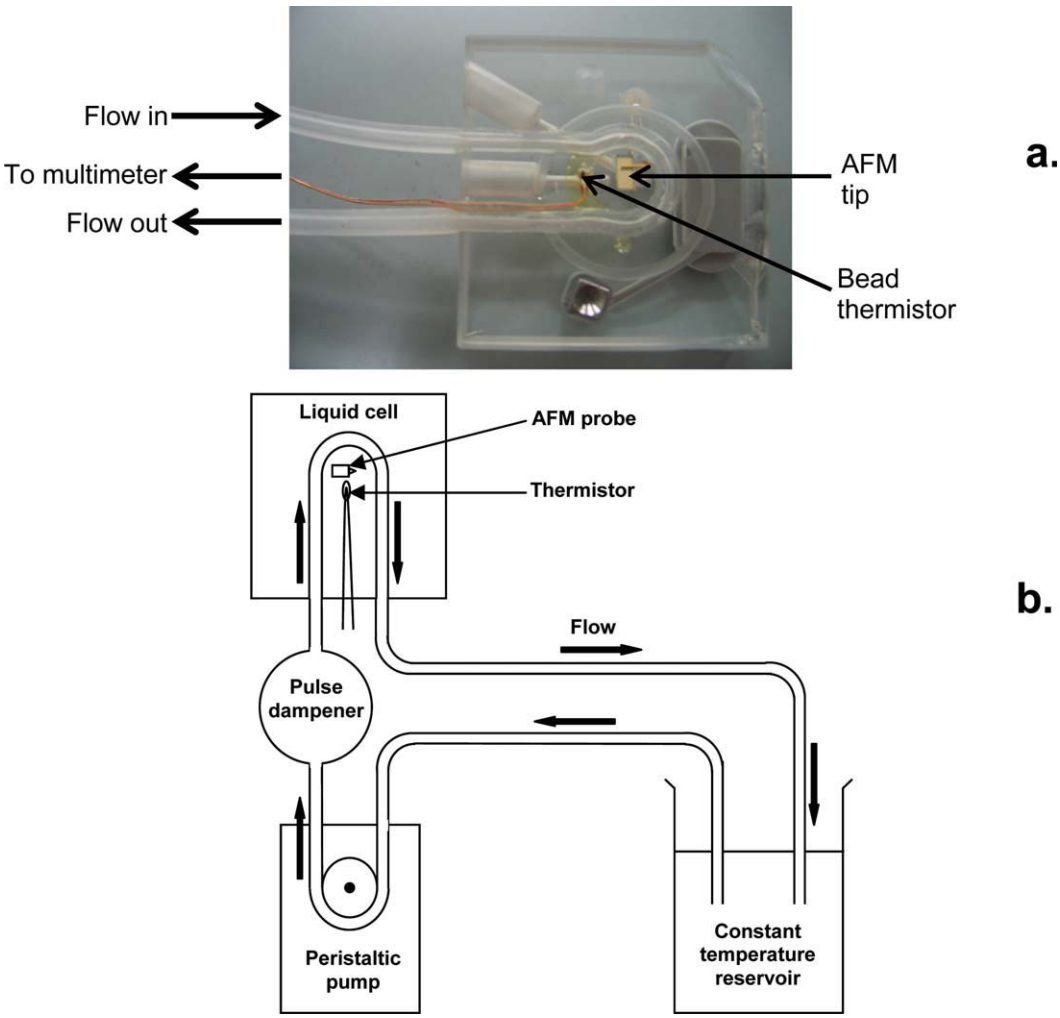

Fig. 2. **a**: A modified liquid cell to enable heating/cooling of liquid samples; (**b**) Schematic of the heating/cooling mechanism. [Color figure can be viewed in the online issue, which is available at wileyonlinelibrary.com.]

The DSU monolayer was first exposed for 10 min to a solution of R6 in the DTT containing solvent to allow the DSU succinimide groups to bind with primary amine groups of the peptide, while the peptides remained in a monomeric state. After this, the substrates were washed with excess quantities of the solvent without the DTT present. This was to remove the DTT so that thiol bonds could be formed between the cysteine residues of the peptides and the gold coated AFM probes.

Silicon nitride AFM probes of nominal spring constant $\sim$0.06 Nm^{-1} were first coated with $\sim$1 nm of chromium followed by $\sim$10 nm of gold by evaporation. Cantilever spring constants were calibrated using the reference cantilever method (Torii et al., 1996). Experiments were conducted over a z-range of 200 nm at a rate of 0.2 Hz, i.e., at a speed of 80 nms^{-1}, in all cases. Control experiments were carried out using coated and uncoated probes on TSG and DSU surfaces.

Room temperature experiments were performed in solution in the standard proprietary liquid cell of a Digital Instruments Multimode AFM. Experiments at controlled temperatures were performed using the modified liquid cell system illustrated schematically in Figure 2. A channel was carefully cut into a standard Multimode liquid cell which, with entry and exit points at the front of the cell, connected to the existing groove for the silicon rubber O-ring. This allowed a silicon rubber tube to be inserted from the front of the cell, around the cantilever holder, and back out of the front of the cell. Hot or cold water was circulated though the silicon rubber tube using a Cole-Parmer peristaltic pump in order to raise or lower the temperature of the imaging liquid. The temperature of the imaging liquid was measured using a bead thermistor placed close to the AFM cantilever. Careful control of the temperature of the circulating water and the speed of the peristaltic pump allowed the imaging liquid temperature to be kept stable to within $\pm$ 0.5°C. A pulse dampener was included between the peristaltic pump and AFM to eliminate vibrations being transmitted to the AFM via the tubing. The same temperature control system has also been successfully used to study the effect of temperature on the dissolution of

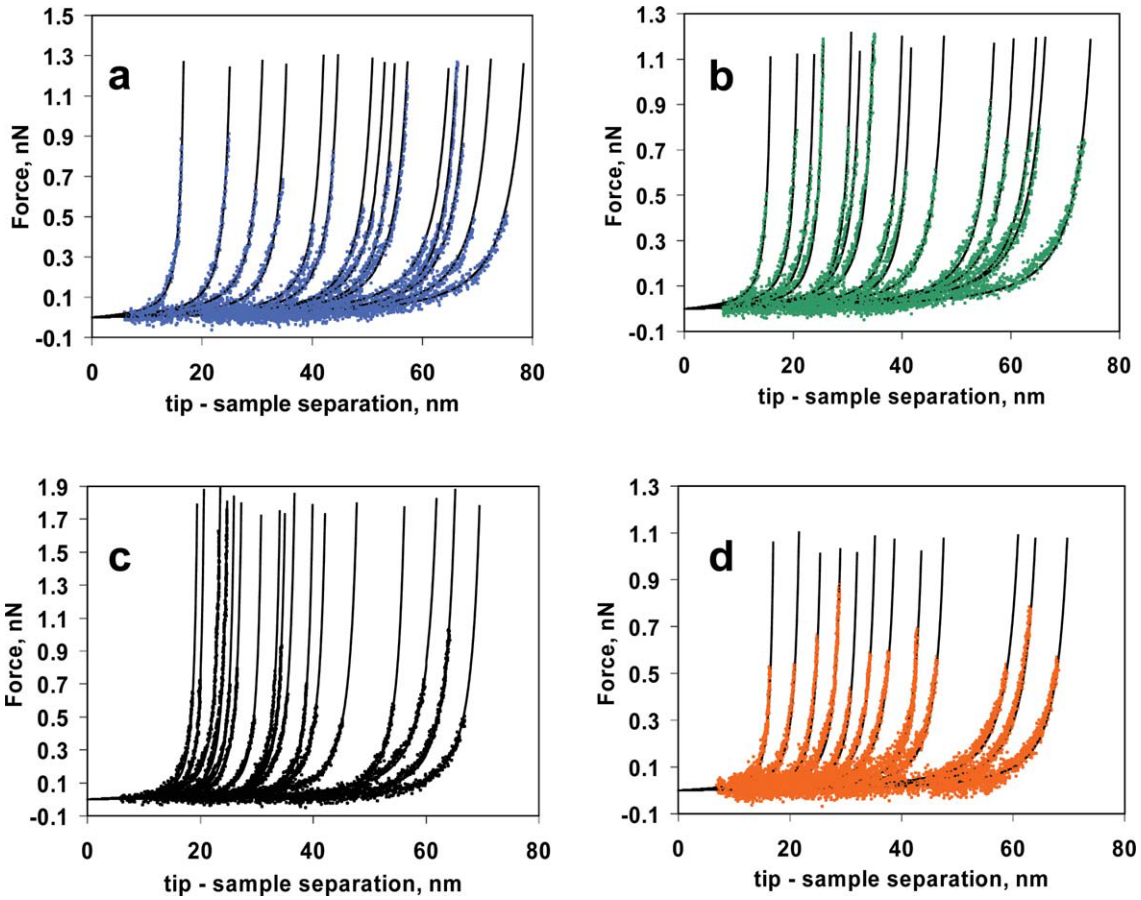

Fig. 3. Examples of force curves obtained with R6 (**a**) $NaHCO_3$ in H_2O at 8°C, (**b**) $NaHCO_3$ in H_2O at 25°C, (**c**) $NaHCO_3$ in D_2O at 25°C, (**d**) $NaHCO_3$ in D_2O at 45°C. [Color figure can be viewed in the online issue, which is available at wileyonlinelibrary.com.]

phyllosilicate minerals by real time AFM imaging (McMaster et al., 2008).

Data obtained with the AFM were corrected to obtain plots of force as a function of peptide extension. The point of zero extension was taken as the point of hard contact between the cantilever tip and the substrate and the sensitivity of the AFM's photodiode detection system to the bending cantilever was determined from the region of constant gradient on the approach curve after contact. Force values were calculated from the measured cantilever deflection and force constant and using Hooke's law.

Values for the persistence length of the molecule were extracted by fitting the corrected experimental data with the WLC force-extension model (Bustamante et al., 1994):

$$F = \frac{k_B T}{p} \cdot \left(\frac{1}{4(1 - x/L_c)} - \frac{1}{4} + \frac{x}{L_c} \right) \quad (1)$$

where F is the applied force, x is the extension of the molecule, p is the persistence length, L_c is the contour length and k_B and T are the Boltzmann constant and temperature.

A nonlinear regression routine was used to find the best fit to the experimental data and return values for p and L_c.

RESULTS AND DISCUSSION

Figure 3 shows typical examples of force-distance curves obtained for the R6 molecule in the H_2O and D_2O based solvents at various temperatures. The data is well represented by the WLC model [Eq. (1), solid lines] in all cases. The force initially increases slowly with extension as the molecule unfolds and then begins to asymptote as bonds become stretched. The experimental force curve ends when the force becomes great enough to rupture a bond and the link between the AFM probe and the substrate is broken.

The range of forces found at the point of maximum extension, i.e., bond rupture, is generally between 0.5 and 1.5 nN, consistent with the force required to break a covalent bond (Grandbois et al., 1999). The smooth and continuous nature of the curves up until the rupture points indicates continuous extension of the peptide chains and indicates that no conformational transitions occur during the stretching process.

The maximum stretch lengths achieved are of ~70 to 80 nm, similar to the expected contour length of the R6 molecule, which is estimated at ~77 nm based on 3.8 Å per amino acid residue. Ruptures occurring at shorter stretches than this are likely to be due to binding of the peptide to the DSU layer via amide groups associated with glutamine residues, as opposed to the N-terminal

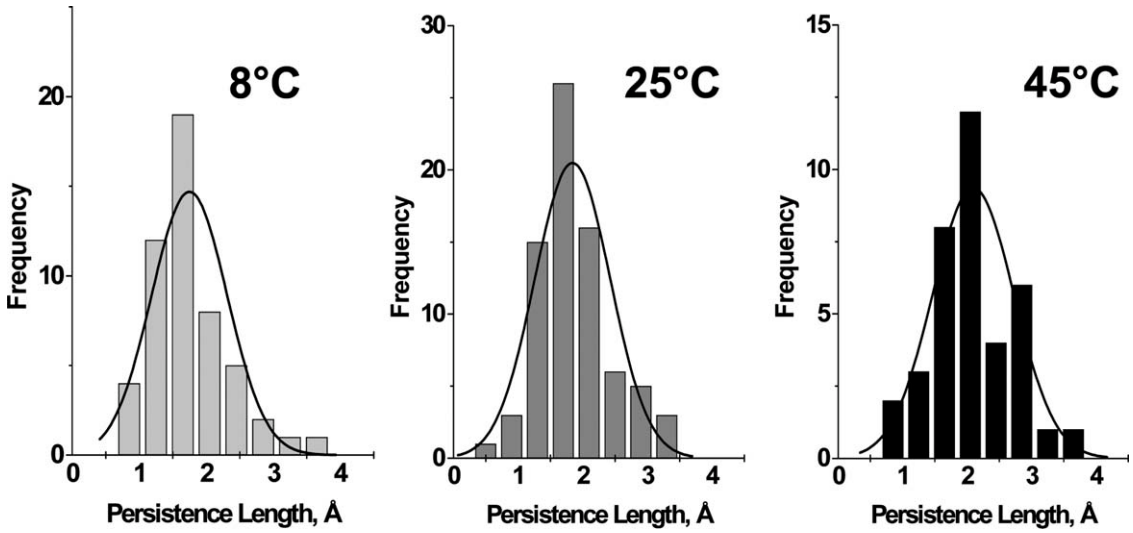

Fig. 4. Persistence length distributions for R6 in an H_2O based solvent at the temperatures indicated.

group. Although the exposed succinimide group of the DSU monolayer has the highest reactivity towards primary amine groups (Wagner et al., 1996), there is also some reactivity with amide groups. In the R6 molecule, there are 66 amide groups on the glutamine residues and only one primary amine (the N-terminus), so there is a high chance that some molecules could have been tethered in this way. Such tethering is not expected to affect the determination of persistence length, however, due to the highly regular and repetitive nature of the peptide. Indeed, we find no correlation between contour length and persistence length in our data.

Figure 4 shows histograms of the persistence length for R6 in a 20 mM solution of $NaHCO_3$ in H_2O at the temperatures indicated. The solid lines show normal distributions determined from the means and standard deviations of the data sets. Here, we see a slight increase in the persistence length with increasing temperature. Incremental increases in the temperature cause increases in the persistence length of fairly low statistical significance (*t*-tests give 60% significance for the increase from 8°C to 25°C and 95% significance for the increase from 25 to 45°C). However, there is a total increase in persistence length of ~17% between 8 and 45°C, which is significant to >99% confidence. This increase in persistence length indicates a significant stiffening of the molecular backbone, or a significant reduction in flexibility. Associated with this would be an expansion or unfolding of the molecule, which could be expected from thermodynamic considerations as the solvent quality should be significantly improved at the elevated temperature. This is also consistent with the findings of previous authors that lower forces are required to extend biological molecules at higher temperatures (Janovjak et al., 2003; Law et al., 2003; Schlierf and Rief, 2005; Taniguchi et al., 2008).

Similar histograms for the persistence lengths found for R6 in the D_2O based solvent are displayed in Figure 5. In this case, there is a very marked increase in persistence length on each increment in temperature. In fact, *t*-tests show >99% confidence in the increase in the mean persistence length at each temperature increase. The total increase in persistence length between 8 and 45°C is ~ 40%.

The mean value of the persistence length is plotted as a function of temperature for R6 in both the H_2O and D_2O based solvents in Figure 6. The error bars represent ± 2 standard errors in the mean, i.e., a 98% confidence interval either side of the data point. The difference in persistence lengths found in H_2O and D_2O at 8°C are statistically insignificant. However, at 25°C the difference is significant to >98% confidence. At 45°C, the difference is significant to >99% confidence. The persistence length increases with temperature in both the H_2O and D_2O based solvents; however, the increase is much more rapid with temperature in the D_2O solution. The gradient of the linear fit to the D_2O data points is roughly double that of the fit to the H_2O data points. At 45°C the persistence length in D_2O is ~25% greater than in H_2O.

Hence, the present results seem to show that the peptide molecule expands and thermally softens to a significantly greater degree when solvated in D_2O compared with in H_2O. This is in contrast to the results of Dougan et al. (2008) for the effect of D_2O on the stability of the I27 module of titin, who found a greater force was required to unfold the protein in D_2O than in H_2O at ambient temperature. Dougan et al. explain this as being due to an enhancement of the hydrophobic effect in D_2O.

Cioni and Strambini (2002) found a general trend of structure expansion of various proteins with temperature in both H_2O and D_2O. However, in general at a given temperature, the secondary structure was relatively more tightly folded when proteins were solvated in D_2O compared with H_2O, consistent with the findings of Dougan et al. for I27. This tighter folding of the protein would imply a lower persistence length in D_2O; an effect that was generally amplified at higher temperatures in the work of Cioni and Strambini. This appears contrary to the currently presented results, however, not all the proteins studied by Cioni and

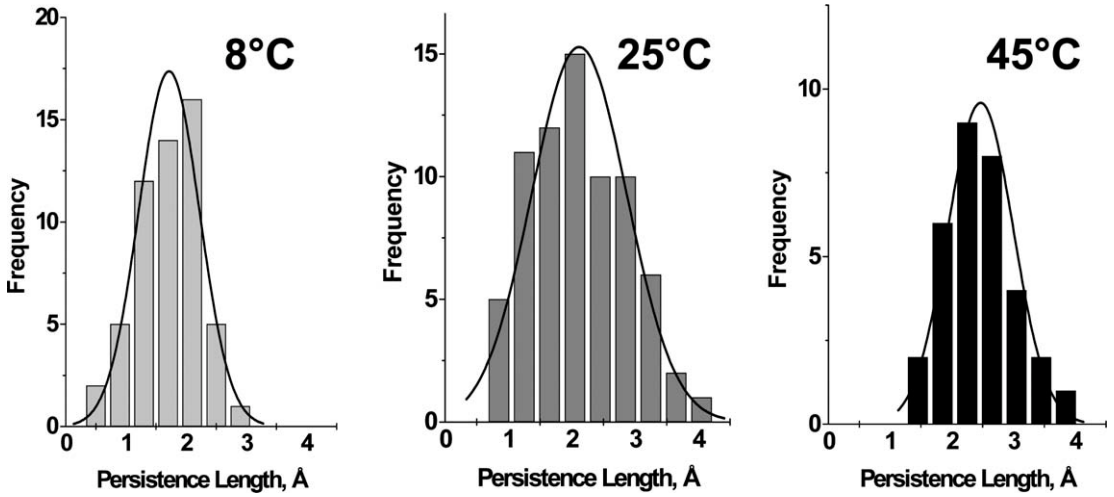

Fig. 5. Persistence length distributions for R6 in a D_2O based solvent at the temperatures indicated.

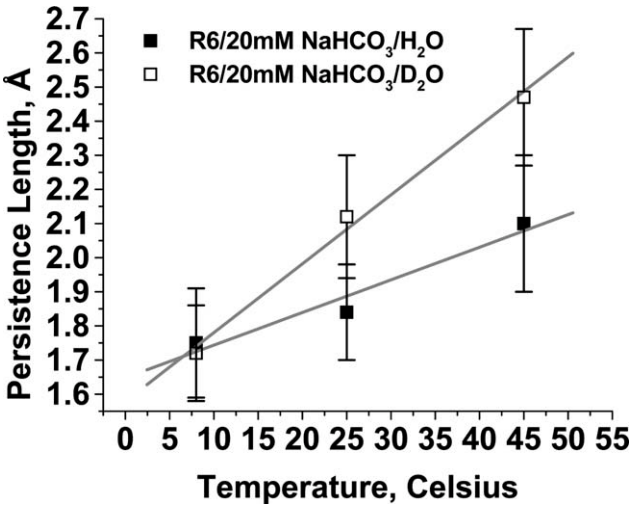

Fig. 6. Persistence length as a function of temperature for R6 in H_2O and D_2O based solvents.

Strambini followed this general trend. Some of the proteins (e.g., superoxide dismutase (SOD) and Cd-azurin (CdAz)) showed no relative changes with temperature (i.e., the structure expansion with temperature was essentially the same in both H_2O and D_2O). The protein dimeric alcohol dehydrogenase (LADH) actually showed the opposite trend, with a greater degree of expansion with increasing temperature when solvated in D_2O than in H_2O (as observed with the R6 peptide).

Parker and Clarke (1997) suggest the hydrophobic interaction is the dominant mechanism in the enhancement of protein structure stability, due to the increased strength of the solvent–solvent hydrogen bond in D_2O. This enhances solvent–solvent interactions at the expense of solvent–solute interactions, leading to a greater energetic favorability of burying hydrophobic residues and therefore leading to tighter protein folding. However, the R6 molecule is largely hydrophilic with very few nonpolar amino acid residues. It is possible that in this case the dominant effect of D_2O is to increase the backbone persistence length due to the increased strength of backbone hydrogen bonding because of isotopic substitution of hydrogen by deuterium (Scheiner and Cuma, 1996). Extra rigidity may also be conferred to the peptide structure by stronger hydrogen bonding between backbone amides and amide side chains of glutamine residues, or by stronger hydrogen bonding between amide side chains.

In summary, single molecule AFM force spectroscopy has revealed statistically significant differences for the persistence length of the elastic peptide R6 solvated in either H_2O or D_2O. Although at low temperature there is little difference in the peptide structure in either solvent, with increasing temperature the persistence length increases more rapidly in D_2O than it does in H_2O. In the case of R6, this difference is most likely to be caused by a stiffening of the peptide backbone due to the increase in strength of backbone hydrogen bonds due to isotopic substitution of hydrogen by deuterium. These results may be of great importance to researchers studying peptide or protein conformations using spectroscopy techniques in which samples are solvated by D_2O.

REFERENCES

Bouchiat C, Wang MD, Allemand JF, Strick T, Block SM, Croquette V. 1999. Estimating the persistence length of a worm-like chain molecule from force-extension measurements. Biophys J 76:409–413.

Bustamante C, Marko JF, Siggia ED, Smith S. 1994. Entropic elasticity of lambda-phage DNA. Science 265:1599–1600.

Chelgren BW, Creamer TP. 2004. Effects of H_2O and D_2O on polyproline II helical structure. J Am Chem Soc 126:14734–14735.

Cioni P, Strambini GB. 2002. Effect of heavy water on protein flexibility. Biophys J 82:3246–3253.

Dougan L, Koti ASR, Genchev G, Lu H, Fernandez JM. 2008. A single-molecule perspective on the role of solvent hydrogen bonds in protein folding and chemical reactions. ChemPhysChem 9:2836–2847.

Feeney KA, Wellner N, Gilbert SM, Halford NG, Tatham AS, Shewry PR, Belton PS. 2003. Molecular structures and interactions of repetitive peptides based on wheat glutenin subunits depend on chain length. Biopolymers 72:123–131.

Forbes JG, Jin AJ, Ma K, Gutierrez-Cruz G, Tsai WL, Wang K. 2005. Titin PEVK segment: Charge-driven elasticity of the open and flexible polyampholyte. J Muscle Res Cell Motil 26:291–301.

Grandbois M, Beyer M, Rief M, Clausen-Schaumann H, Gaub HE. 1999. How strong is a covalent bond? Science 283:1727–1730.

Hegner M, Wagner P, Semenza G. 1993. Ultralarge atomically flat template-stripped Au surfaces for scanning probe microscopy. Surf Sci 291:39–46.

Janovjak H, Kessler M, Oesterhelt D, Gaub H, Muller DJ. 2003. Unfolding pathways of native bacteriorhodopsin depend on temperature. EMBO J 22:5220–5229.

Law R, Liao G, Harper S, Yang GL, Speicher DW, Discher DE. 2003. Pathway shifts and thermal softening in temperature-coupled forced unfolding of spectrin domains. Biophys J 85:3286–3293.

Lee GU, Chrisey LA, Colton RJ. 1994. Direct measurement of the forces between complementary strands of DNA. Science 266:771–773.

Markus Y, Ben-Naim A. 1985. A study of the structure of water and its dependence on solutes, based on the isotope effects on solvation thermodynamics in water. J Chem Phys 83:4744–4759.

McIntire TM, Lew EJL, Adalsteins AE, Blechl A, Anderson OD, Brant DA, Kasarda DD. 2005. Atomic force microscopy of a hybrid high-molecular-weight glutenin subunit from a transgenic hexaploid wheat. Biopolymers 78:53–61.

McMaster TJ, Smits MM, Haward SJ, Leake JR, Banwart S, Ragnarsdottir KV. 2008. High-resolution imaging of biotite dissolution and measurement of activation energy. Mineralogical Mag 72:115–120.

Miles MJ, Carr HJ, McMaster T, l'Anson KJ, Belton PS, Morris VJ, Field JM, Shewry PR, Tatham AS. 1991. Scanning tunneling microscopy of a wheat gluten protein reveals details of an unusual supersecondary structure. Proc Natl Acad Sci USA 88:68–71.

Milne JS, Mayne L, Roder H, Wand AJ, Englander SW. 1998. Determinants of protein hydrogen exchange studied in equine cytochrome c. Protein Sci. 7:739–745.

Moy VT, Florin E-L, Gaub HE. 1994. Intermolecular forces and energies between ligands and receptors. Science 266:257–259.

Nemethy G, Scheraga HA. 1964. Structure of water and hydrophobic bonding in proteins. IV. The thermodynamic properties of liquid deuterium oxide. J Chem Phys 41:680–689.

Parchment O, Shewry PR, Tatham AS, Osguthorpe DJ. 2001. Molecular modeling of unusual spiral structure in elastomeric wheat seed protein. Cereal Chem 78:658–662.

Parker MJ, Clarke AR. 1997. Amide backbone and water-related H/D isotope effects on the dynamics of a protein folding reaction. Biochemistry 36:5786–5794.

Rief M, Oesterhelt F, Heymann B, Gaub HE. 1997. Single molecule force spectroscopyon polysaccharides by atomic force microscopy. Science 275:1295–1297.

Scheiner S, Cuma M. 1996. Relative stability of hydrogen and deuterium bonds. J Am Chem Soc 118:1511–1521.

Schlierf M, Rief M. 2005. Temperature softening of a protein in single-molecule experiments. J Mol Biol 354:497–503.

Shewry PR, Tatham AS. 1990. The prolamin storage proteins of cereal seeds: Structure and evolution. Biochem J 267:1–12.

Taniguchi Y, Brockwell DJ, Kawakami M. 2008. The effect of temperature on mechanical resistance of the native and intermediate states of I27. Biophys J 95:5296–5305.

Torii A, Sasaki M, Hane K, Okuma S. 1996. A method for determining the spring constant of cantilevers for atomic force microscopy. Meas Sci Technol 7:179–184.

Wagner P, Hegner M, Kernen P, Zaugg F, Semenza G. 1996. Covalent immobilization of native biomolecules onto Au(111) via *N*-hydroxysuccinimide ester functionalized self-assembled monolayers for scanning probe microscopy. Biophys J 70:2052–2066.